EGTRIB Journal
JOURNAL OF
THE EGYPTIAN SOCIETY OF TRIBOLOGY
VOLUME 21, No. 2, April 2024, pp. 1 – 14 **ISSN 2090 - 5882**
(Received January 4. 2024, Accepted in final form March 9. 2024) **jest.journals.ekb.eg**

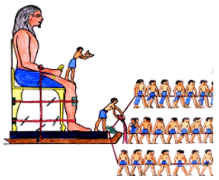

DEVELOPMENT OF DIRECT CURRENT TRIBOELECTRIC NANOGENERATOR

Ali A. S.[1], Al-Kabbany A. M.[2], Ali W. Y.[2] and Atia A. M.[3,4]

[1]Mechanical Engineering Dept., Faculty of Engineering, Suez Canal University,
[2]Production Engineering and Mechanical Design Department, Faculty of Engineering, Minia University, P. N. 61111, El-Minia,
[3]Department of Mechanical Design and Production Engineering, Faculty of Engineering, Assiut University,
[4]Mechanical Engineering Department, Faculty of Engineering, Sphinx University, Assiut, EGYPT.

ABSTRACT

The present work proposes five types of DC TENG based on electrostatic breakdown to generate direct current to be applied in small electronic appliances.

Triboelectric nanogenerator (TENG) is a technology that combines electrostatic induction and triboelectrification to harvest energy. The output of the TENG is an alternating current (AC) that needs a rectifier to obtain a direct current (DC). Recently, direct current triboelectric nanogenerator DC TENG has been developed based on the combination of triboelectrification and electrostatic breakdown. The present work proposes five types of DC TENG to generate direct current to be applied in small electronics.

It was revealed that the voltage harvested by the DC-TENG resulted from the triboelectrification and electrostatic breakdown and generated direct current passed through the electrodes and Al surface. It was observed that voltage displayed maximum values at a certain value of the contact area of the electrodes. When Cu electrodes were replaced by Al ones, voltage showed higher voltage at the controlled length of the electrodes. Besides, the oily sliding of Cu on PTFE displayed a drastic voltage decrease, while the oily sliding of Cu on Kapton increased the voltage. Water-wet sliding of Al on PTFE showed higher voltage values than the dry one. While, Al sliding on PMMA at water conditions presented a remarkable voltage increase, especially for the connected two electrodes.

KEYWORDS

Direct current, triboelectric nanogenerator, Kapton, polytetrafluoroethylene, polymethyl methacrylate.

INTRODUCTION

The technology of harvesting mechanical energy and converting it into electrical one is called energy harvesting. Triboelectric nanogenerator (TENG) can harvest mechanical energy by contact/separation mechanism and sliding of two material surfaces on each other. Combining contact electrification and electrostatic induction produces electrical current.

Direct current triboelectric nanogenerator, (DC-TENG), can generate electric current during sliding. That behavior facilitates its application on the surface of the electronic skin (e-skin), [1 - 6]. Sliding of DC-TENG increased the ESC magnitude on the friction surface and induced an electrostatic field acting in the gap between the friction surface and electrode. It was proposed to insert two charge-collecting electrodes at the rear and front of the friction electrode to increase the output voltage. The DC-TENG was recommended to be applied in the design of e-skin.

It was found that the conventional TENG generally produced alternating current (AC), which needs electrical circuits to rectify its output. The application of the TENG limits the harvested energy. The requirements increased to apply direct-current TENGs, [7 - 13]. It was revealed that the semiconductor-based DC TENG can produce high density DC output, [8 - 15]. However, normal load and sliding frequency enhanced the triboelectric output. It was revealed that polyurethanes (PU) and ethylenetetrafluoroethylene (ETFE) present significant output for DC-TENG, [16]. It was developed by solving the factors influencing its performance such as friction coefficient, surface charge density, leakage current, and breakdown charge density, [17, 19], by liquid lubrication, [20] and material selection, [21 - 25], where surface charge (ESC) increased. Generation of feedback electric signal due to sliding on the object surface is essential in the design of e-skin, [26 - 30]. Besides, TENG performed by triboelectrification and electrostatic induction were utilized, [31 - 40].

The present work proposes five types of DC TENG based on electrostatic breakdown to generate direct current to be applied in small electronic appliances.

EXPERIMENTAL

The proposed five types of the DC TENG are illustrated, and their performance is discussed in the present work. The proposed first DC TENG is shown in Fig. 1, a. PTFE film 20 μm thickness was adhered to a PMMA cube of 30 × 30 × 30 mm^3. The second friction surface was a PMMA sheet of 3.0 mm thickness. On the front and rear edges, two copper (Cu) films of 20 μm thickness were connected to the Cu film representing the charge collecting electrode (CCE). The distribution of the Cu film on the PTFE surface is illustrated in Fig. 1, b. The second proposed TENG consisted of the two friction surfaces one slide on the other. The slider surface was coated by PTFE film adhered to a PMMA cube, where two electrodes of aluminum (Al) film of 25 μm thickness representing the output terminals of the TENG are installed on both sides of the slider to collect ESC, Fig. 2, a. The length of the Al electrode ranged between 4 and 24 mm while the width was 10 mm. Figure 2, b shows the 3D schematic diagram of the second TENG.

The third proposed DC TENG contained Cu film of 20 µm thickness adhered on one surface of the PMMA cube of 30 × 30 × 30 mm^3 to represent the sliding electrode on the dielectric friction surface. Then Cu film of 20 µm thickness, 20 mm width, and 30 mm length was adhered on one surface of the PMMA cube representing the second electrode. The dielectric friction surface was PTFE film of 20 µm thickness adhered on the acrylic substrate, Fig. 3. The fourth proposed TENG had the same construction as the third one except that the dielectric friction surface (PTFE) was replaced by Kapton film of 25 µm thickness, Fig. 4. The fifth TENG is shown in Fig. 5, where the Cu film was replaced by the aluminum film (Al) of 80 µm thickness. The dielectric friction surface was PTFE and PMMA. Load values were ranging between 0.25 and 10.25 N. The sliding distance was 100 mm. Experiments were carried out at dry and lubricated sliding conditions. The lubricant was paraffin oil and water.

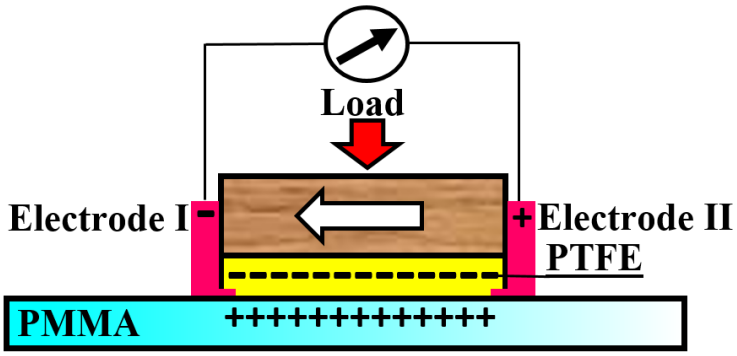

Fig. 1, a Arrangement of the first TENG.

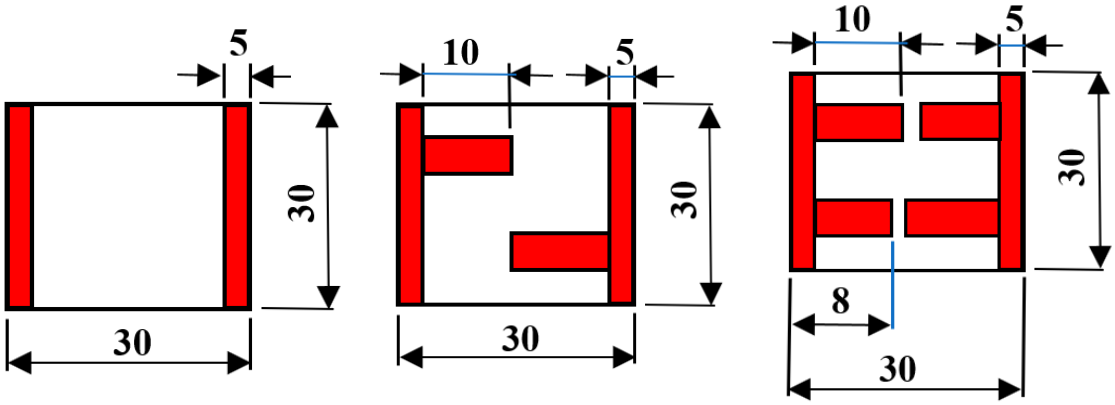

Fig. 1, b Distribution of the electrodes in the sliding surface of PTFE film.

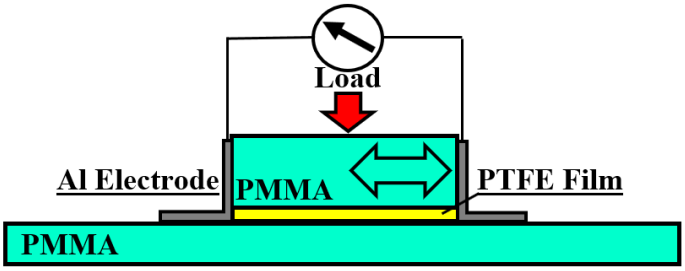

Fig. 2, a Arrangement of The second proposed TENG.

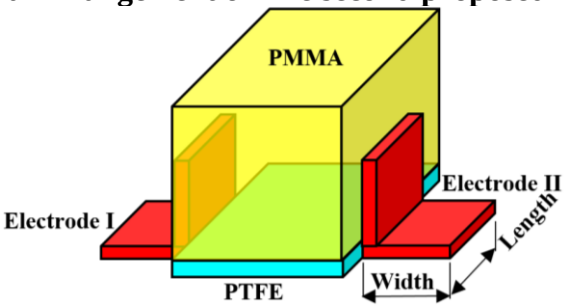

Fig. 2, b 3D Diagram of the second TENG.

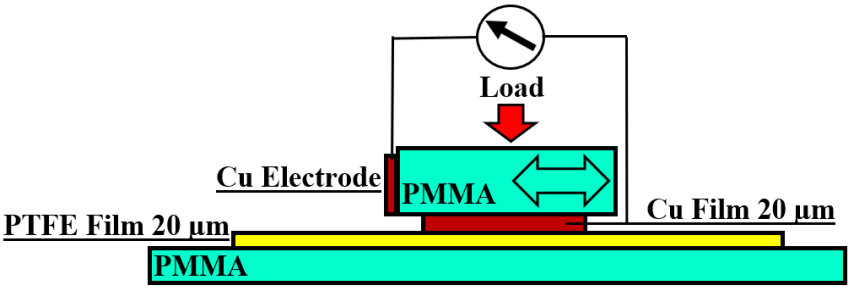

Fig. 3 Arrangement of the third proposed TENG.

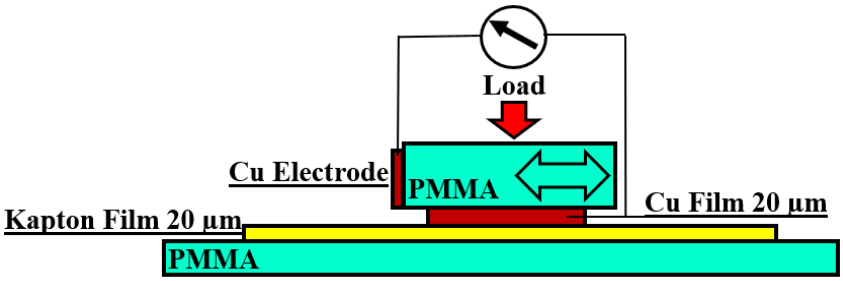

Fig. 4 Arrangement of the fourth proposed TENG.

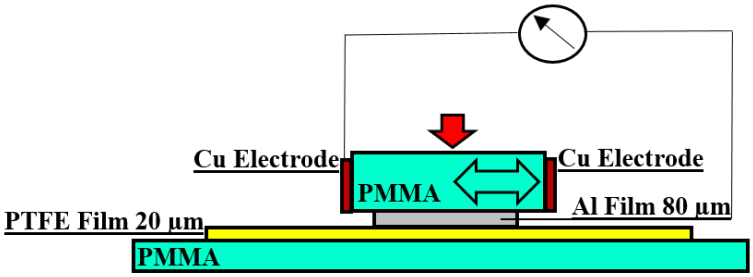

Fig. 5, a Arrangement of the fifth proposed TENG.

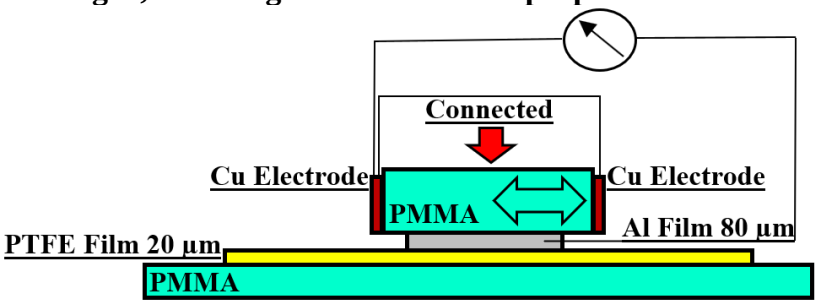

Fig. 5, b Arrangement of the fifth proposed TENG of connected electrodes.

RESULTS AND DISCUSSION

The design of the proposed DC TENG depends on generating DC current from the sliding of the tested materials on each other. The voltage generated from the first DC TENG at dry sliding measured between charge collecting electrodes I and II is shown in Fig. 6. It is seen that voltage slightly increased up to maximum and then slightly decreased with increasing the relative contact area of the electrode. As the applied load increased, the voltage increased due to increasing the contact area. The highest voltage values were measured when the relative contact area was 50 % of the area of PTFE, where the highest value (850 mV) was observed at 10.25 N. Sliding of DC TENG after rinsing the sliding surface by paraffin oil showed the same trend observed for dry sliding, Fig. 7. It is known that using lubricant on the friction surface facilitates the sliding and decrease wear.

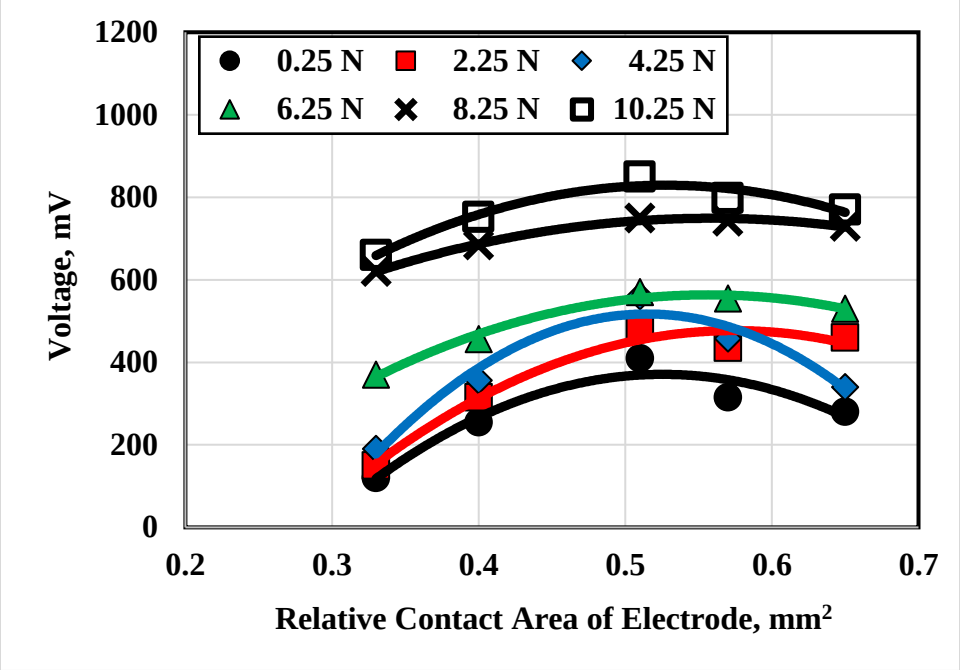

Fig. 6 Voltage generated from the first DC TENG at dry sliding.

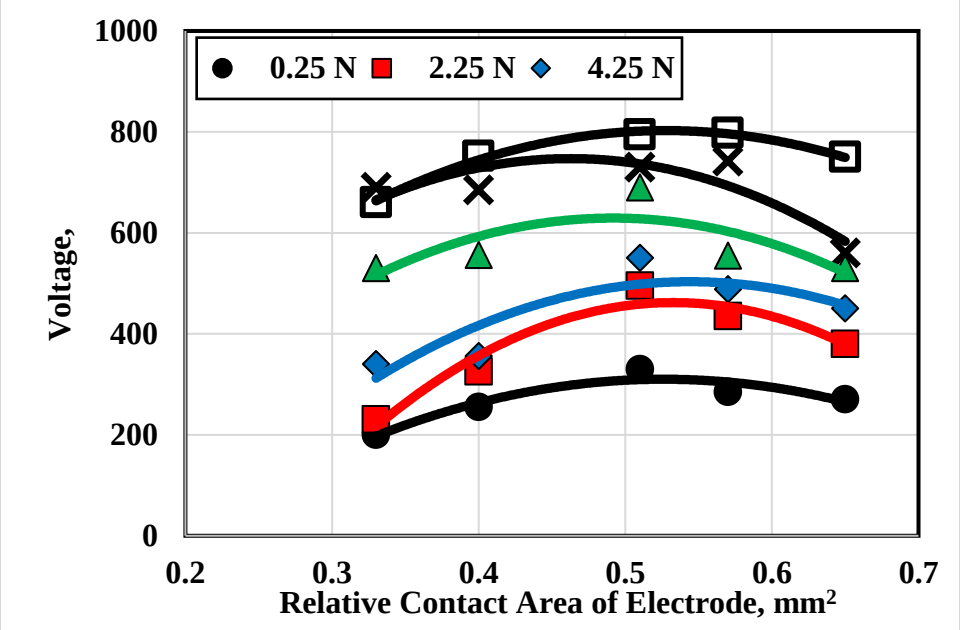

Fig. 7 Voltage generated from the first DC TENG at oil sliding.

The second proposed DC TENG displayed a relatively higher voltage generated at dry sliding, Fig. 8, when the Cu electrodes were replaced by Al ones. Voltage increased up to maximum and then decreased with the increase of the length of the electrodes, where the highest values were observed at the length of an electrode of 12

– 16 mm and 10 mm width. The highest recorded voltage was 1100 mV at 10.25 N load.

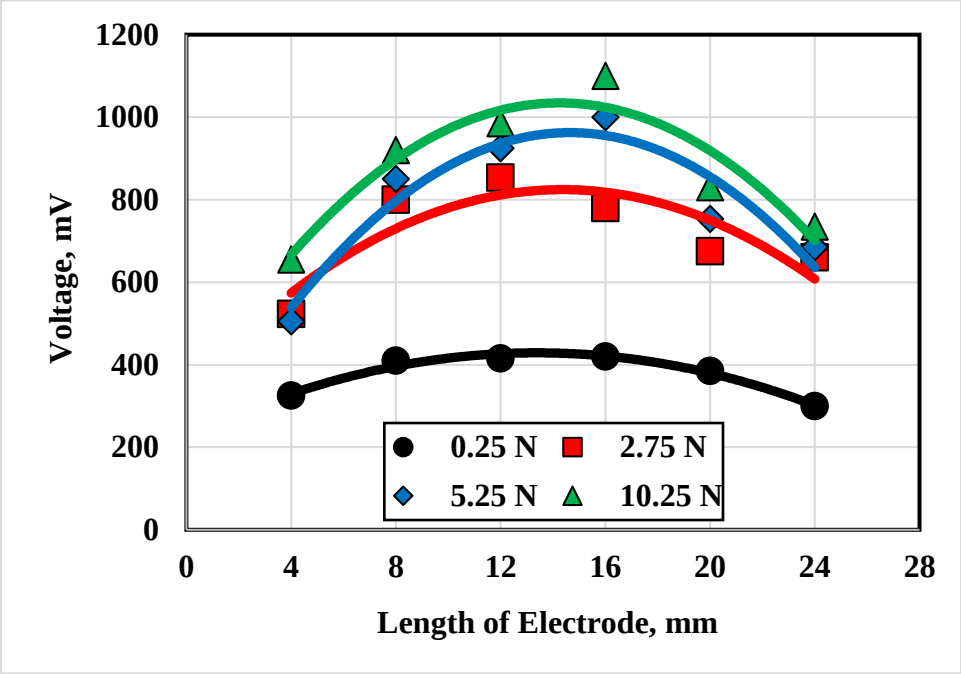

Fig. 8 Voltage generated from the second DC TENG at dry sliding.

The third proposed DC TENG at dry sliding, Fig. 9, showed slight voltage increase with increasing the length of the electrodes. Compared to the output of the first DC TENG, it is observed that the voltage output displayed by the third TENG was lower than that measured for the first TENG. At oily sliding, the voltage drastically decreased, Fig. 10. It seems that the voltage decrease was due to the separation of the two sliding surfaces (Cu/PTFE) that limited the generation of ESC, where the highest voltage value did not exceed 350 mV.

The voltage generated from the fourth DC TENG at dry and oily sliding versus the length of the electrodes for Cu sliding on Kapton is illustrated in Figs. 11, 12. At dry sliding, Fig. 11, the voltage showed a drastic decrease compared to sliding on PTFE. In contradiction to that, oily sliding, Fig. 12, represented relatively higher values than that shown in dry sliding.

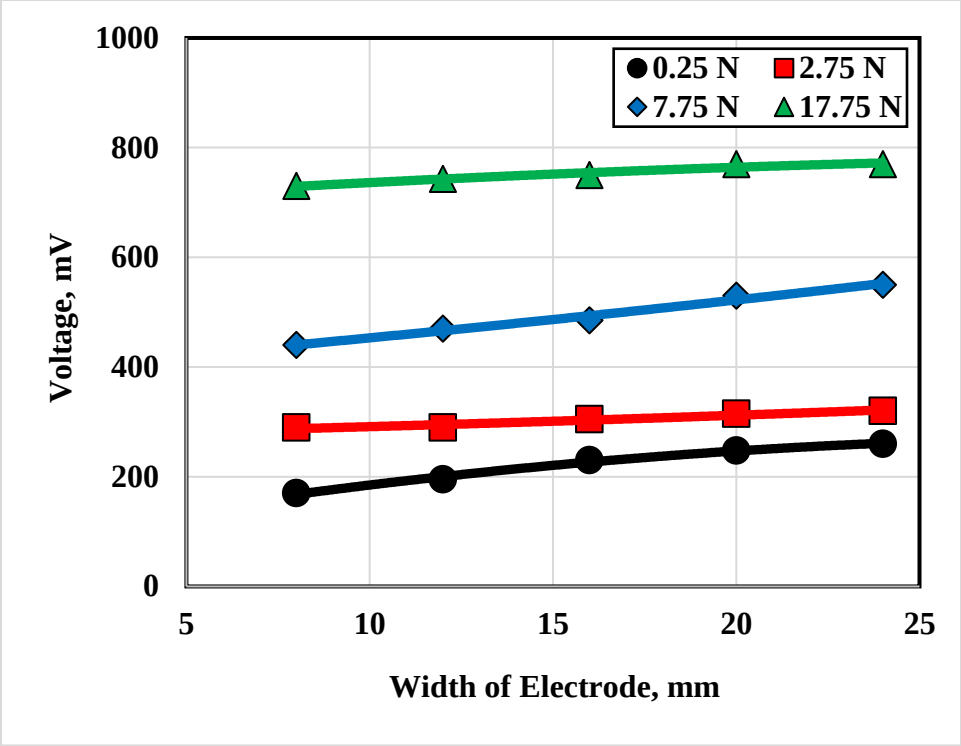

Fig. 9 Voltage generated from the third DC TENG at dry sliding.

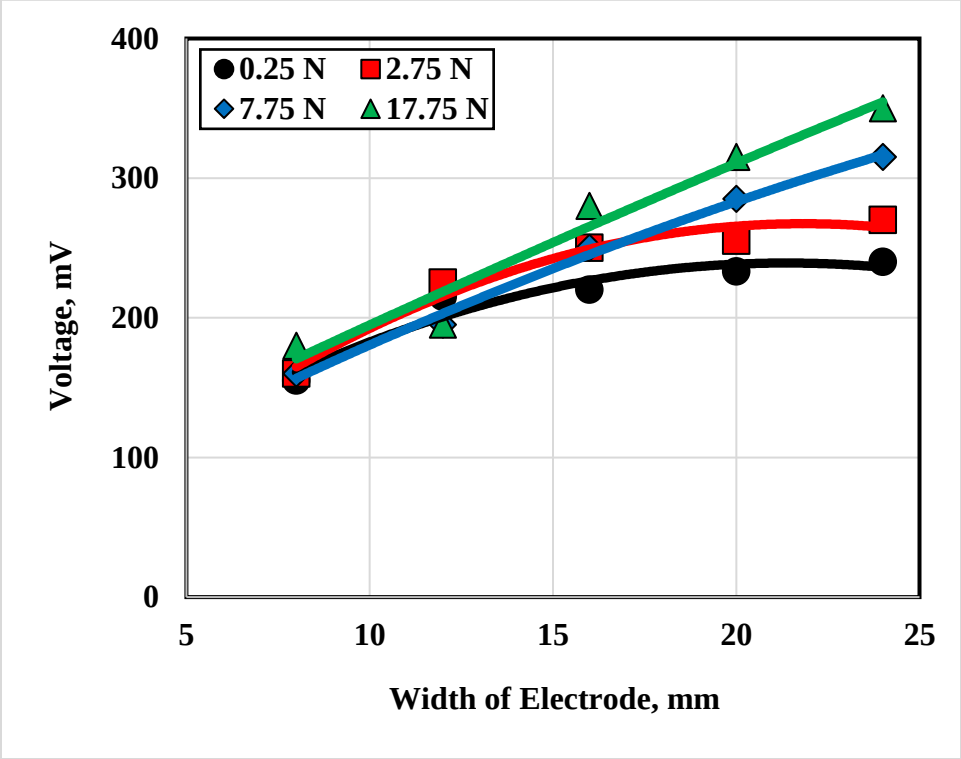

Fig. 10 Voltage generated from the third DC TENG at oily sliding.

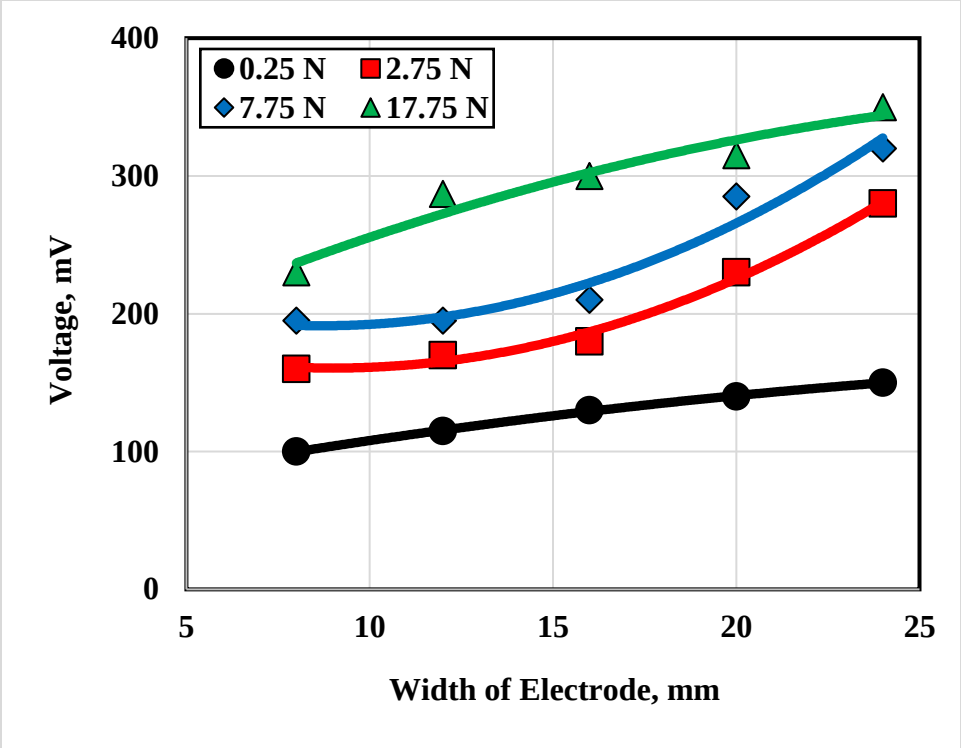

Dry **Fig. 11 Voltage generated from the fourth DC TENG at dry sliding.**

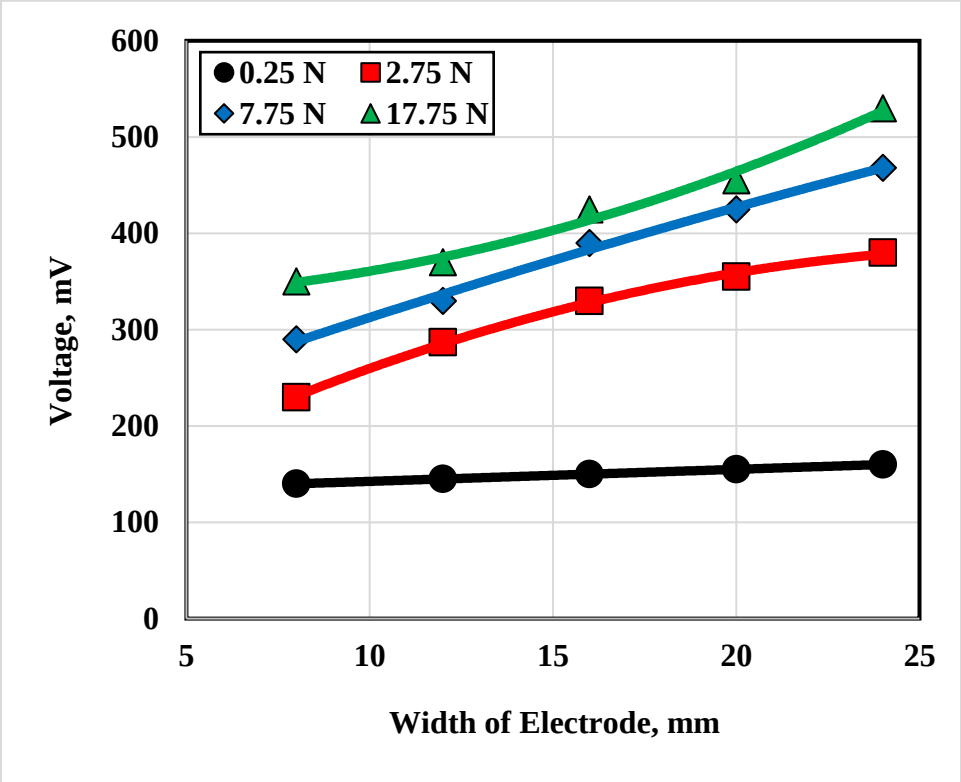

Fig. 12 Voltage generated from the fourth DC TENG at oily sliding.

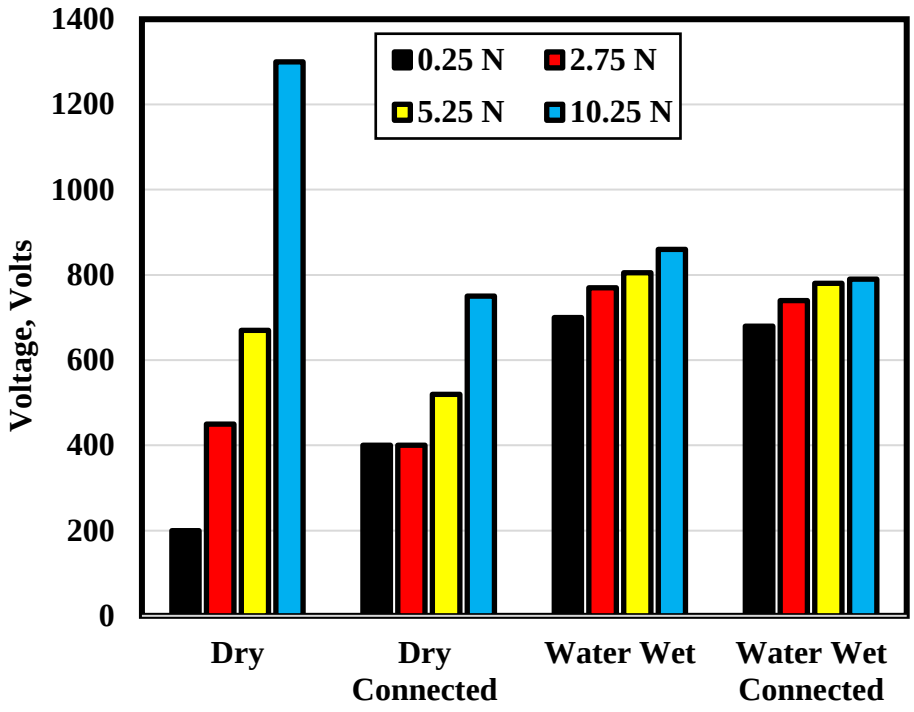

Fig. 13 Voltage generated from the fifth DC TENG for Al sliding on PTFE.

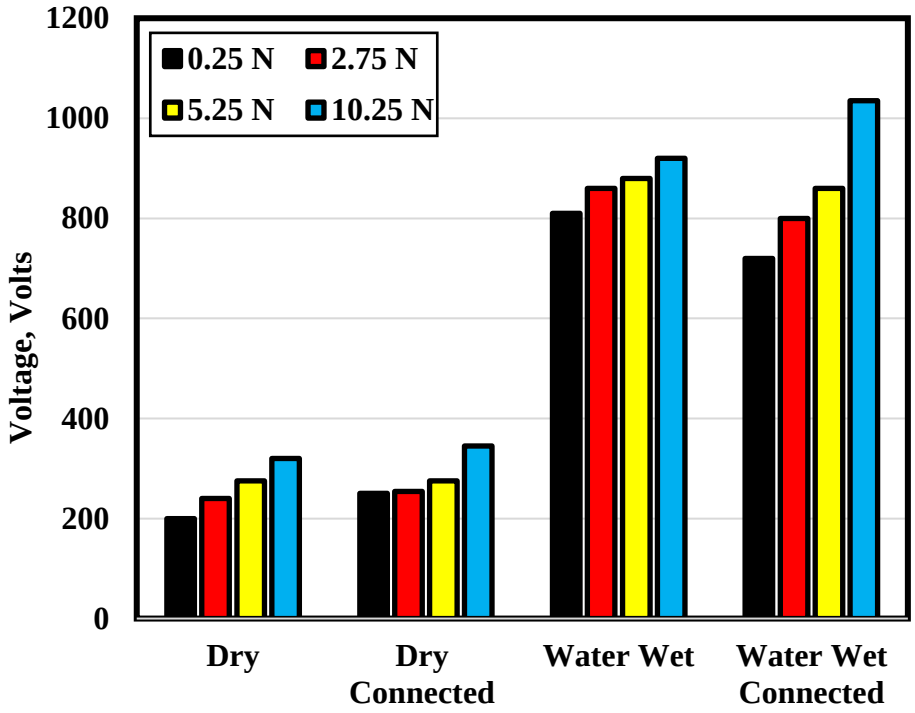

Fig. 14 Voltage generated from the fifth DC TENG for Al sliding on PMMA.

The voltage difference harvested by the fifth DC-TENG is illustrated in Fig. 13, where the Al film slides on PTFE film at dry and water wet conditions. The measurements were performed also when the two electrodes were connected. The highest voltage value was observed at dry sliding and 10.25 N load. Besides, connecting the two electrodes did not enhance the voltage. Generally, water wet sliding displayed relatively higher voltage values than dry sliding. It seems that the water film on the sliding surface enhanced the output performance of the DC TENG and conducted the ESC to the electrodes. The effect of lubricating the sliding surface with water is clearly shown when PTFE film was replaced by PMMA, Fig. 14, where a remarkable voltage increase was observed in the condition of water wet sliding. Besides, connecting the two electrodes displayed the highest voltage (1035 mV) at the highest load (10.25 N). The voltage harvested by the DC-TENG resulted from the triboelectrification and electrostatic breakdown, where direct current passed through the electrodes and Al surface due to the electrostatic field. The gap between the electrodes and PMMA was ionized and consequently direct current flew in the external circuit. While the Al surface slides forward, the ESC is transmitted from PMMA to the electrode. Once the Al surface moved forward the electrostatic field induced a negative charge on the surface of PTFE and positive charge on Al surface. In condition of sliding of Al surface on PMMA would induce negative charge on Al surface and positive charge on PMMA surface. The movement of Al surface forward generated ESC continuously resulting in a continuous DC output. The size of the DC-TENG can be compacted to be applicable as a self-powered sensor in electronics.

CONCLUSIONS

1. The present work proposes five types of DC TENG to generate DC current from the sliding of the tested materials.
2. Voltage slightly increased up to maximum then slightly decreased with increasing the relative contact area of the electrode.
3. Increasing the applied load increased voltage due to the increase of the contact area.
4. Replacing the Cu electrodes by Al ones displayed relatively higher voltage at a certain length of the electrodes.
5. Oily sliding of Cu on PTFE drastically decreased the voltage.
6. At dry sliding of Cu on Kapton, the voltage drastically decreased compared to sliding on PTFE. While oily sliding showed relatively higher values than that observed in dry sliding.
7. Water wet sliding of Al on PTFE showed higher voltage values than dry sliding. Sliding at dry and water wet conditions
8. Significant voltage increase was measured for Al sliding on PMMA at water wet conditions. Besides, connecting the two electrodes showed the highest voltage at 10.25 N load.

REFERENCES

1. Massoud M. A., Ali A. S., Al-Kabbany A. M., Ali W. Y., and. El-Shazly M. H., "Electronic Skin Based on Direct Current Triboelectric Nanogenerator", Journal of the Egyptian Society of Tribology, Vol. 20, No. 4, October 2023, pp. 44 – 53, (2023).

2. Massoud M. A., Ali W. Y. and Badran A. H., "Electronic Skin Based on Triboelectrification and Electrostatic Induction", Journal of the Egyptian Society of Tribology, Vol. 20, No. 2, April 2023, pp. 77 – 86, (2023).
3. Zhao Z., Liu D., Li Y., Wang Z. L. and Wang J., "Direct-current triboelectric nanogenerator based on electrostatic breakdown effect", Nano Energy 102, 107745, pp. 1 - 15, (2022).
4. Wang S., Xie Y., Niu S., Lin L., Liu C., Zhou Y. S., Wang Z. L., "Maximum surface charge density for triboelectric nanogenerators achieved by ionized-air injection: Methodology and theoretical understanding", Adv. Mater. 26 (39), pp. 6720 - 6728, (2014).
5. Li Y., Zhao Z., Liu L., Zhou L., Liu D., Li S., Chen S., Dai Y., Wang J. and Wang Z. L., "Improved output performance of triboelectric nanogenerator by fast accumulation process of surface charges", Adv. Energy Mater. 11, 2100050, (2021).
6. Zhang C., Zhou L., Cheng P., Yin X., Liu D., Li X., Guo H., Wang Z. L. and Wang J., "Surface charge density of triboelectric nanogenerators: Theoretical boundary and optimization methodology", Appl, Mater. Today 18, 100496, (2020).
7. Liu Y., Liu W., Wang Z., He W., Tang Q., Xi Y., Wang X., Guo H. and Hu C., "Quantifying contact status and the air-breakdown model of charge-excitation triboelectric nanogenerators to maximize charge density", Nat. Commun. 11 (1) 1599, (2020).
8. He H., Fu Y., Zang W., Wang Q., Xing L., Zhang Y., Xue X., "A flexible self-powered TZnO/PVDF/fabric electronic-skin with multifunctions of tactile-perception, atmosphere-detection and self-clean", Nano Energy 31, pp. 37 - 48, (2017).
9. M. Song, J. Hur, D. Heo, S.-H. Chung, D. Kim, S. Kim, D. Kim, Z.-H. Lin, J. Chung, S. Lee, "Current amplification through deformable arch-shaped film based direct-current triboelectric nanogenerator for harvesting wind energy", Applied Energy 344, 121248, (2023).
10. Han J. Y., Singh H. H., Won S., Kong D. S., Hu Y. C., Ko Y. J., et al., "Highly durable direct current power generation in polarity-controlled and soft-triggered rotational triboelectric nanogenerator", Appl Energy, 314,119006, (2022).
11. Song W-Z, Qiu H-J, Zhang J., Yu M., Ramakrishna S., Wang Z. L., et al., "Sliding mode direct current triboelectric nanogenerators", Nano Energy, 90, 106531, (2021).
12. Liu C., Liu J., Liu J., Zhao C., Shan B., Chen N., et al., "A wind-driven rotational direct
current triboelectric nanogenerator for self-powered inactivation of seawater microorganisms", Mater Today Energy;26:100991, (2022).
13. Wang Y., Huang T., Gao Q., Li J., Wen J., Wang Z. L., et al., "High-voltage output triboelectric nanogenerator with DC/AC optimal combination method", Nano Res, 15, 3239 - 45, (2022).
14. Liu D., Bao J-F, Chen Y-L, Li G-K, Zhang X-S, "Unidirectional-current triboelectric nanogenerator based on periodical lateral-cantilevers", Nano Energy, 74, 104770, (2020).
15. Qiao G., Wang J., Yu X., Jia R., Cheng T., Wang Z. L., "A bidirectional direct current triboelectric nanogenerator with the mechanical rectifier", Nano Energy;79: 105408, (2021).

16. Yang D., Zhan L., Luo N., Liu Y., Sun W., Peng J., Feng M., Feng Y., Wang H., Wang D., "Tribological-behaviour-controlled direct-current triboelectric nanogenerator based on the tribovoltaic effect under high contact pressure", Nano Energy 99, 107370, (2022).
17. Liu J., Goswami A., Jiang K., Khan F., Kim S., McGee R., Thundat T., "Direct-current
triboelectricity generation by a sliding Schottky nanocontact on MoS2 multilayers", Nat. Nanotechnol., 13, pp. 112 - 116, (2018).
18. Xuan Y., Chen H., Chen Y., Zheng H., Lu Y., Lin S., "Graphene/semiconductor heterostructure wireless energy harvester through hot electron excitation", Research 2020, 3850389, (2020).
19. Lin S., Lu Y., Feng S., Hao Z., Yan Y., High A., "Current density direct-current generator based on a moving van der Waals Schottky diode", Adv. Mater. 31, 1804398, (2019).
20. Huang X., Xiang X., Nie J., Peng D., Yang F., Wu Z., Zheng Q., "Microscale Schottky superlubric generator with high direct-current density and ultralong life", Nat. Commun. 12, 2268, (2021).
21. Lu Y., Hao Z., Feng S., Shen R., Yan Y., Lin S., "Direct-current generator based on dynamic PN junctions with the designed voltage output", iScience 22, pp. 58 - 69, (2019).
22. Liu J., Zhang Y., Chen J., Bao R., Jiang K., Khan F., Thundat T., "Separation and quantum tunneling of photo-generated carriers using a tribo-induced field", Matter 1, p. 650 - 660, (2019).
23. Li X., Lu J., Yang S., "Effect of lubricant on tribo-induced phase transformation of Si, Tribol. Lett., 24, pp. 61 - 66, (2006).
24. Cui S., Liu D., Yang P., Liu J., Gao Y., Zhao Z., Zhou L., Zhang J., Wang Z. L., Wang J., "Triboelectric-material-pairs selection for direct-current triboelectric nanogenerators", Nano Energy 112 108509, (2023).
25. Liu D., Yin X., Guo H., Zhou L., Li X., Zhang C., Wang J., Wang Z. L., "A constant current triboelectric nanogenerator arising from electrostatic breakdown", Sci. Adv. 5, eaav6437, (2019).
26. Liu D., Zhou L., Wang Z. L., Wang J., "Triboelectric nanogenerator: from alternating current to direct current", iScience 24, 102018, (2021).
27. Zhao Z., Dai Y., Liu D., Zhou L., Li S., Wang Z. L., Wang J., "Rationally patterned electrode of direct-current triboelectric nanogenerators for ultrahigh effective surface charge density", Nat. Commun. 11, 6186, (2020).
28. Zhou L., Liu D., Zhao Z., Li S., Liu Y., Liu L., Gao Y., Wang Z. L., Wang J., "Simultaneously enhancing power density and durability of sliding-mode triboelectric nanogenerator via interface liquid lubrication", Adv. Energy Mater. 10, 2002920, (2020).
29. Zhao Z., Zhou L., Li S., Liu D., Li Y., Gao Y., Liu Y., Dai Y., Wang J., Wang Z. L., "Selection rules of triboelectric materials for direct-current triboelectric nanogenerator, Nat. Commun. 12, 4686, (2021).
30. Liu D., Zhou L., Li S., Zhao Z., Yin X., Yi Z., Zhang C., Li X., Wang J., Wang Z. L., Hugely enhanced output power of direct-current triboelectric nanogenerators by using electrostatic breakdown effect, Adv. Mater. Technol. 5, 2000289, (2020).

31. Yi Z., Liu D., Zhou L., Li S., Zhao Z., Li X., Wang Z. L., Wang J., "Enhancing output performance of direct-current triboelectric nanogenerator under controlled atmosphere", Nano Energy 84, 105864, (2021).
32. Chen S., Liu D., Zhou L., Li S., Zhao Z., Cui S., Gao Y., Li Y., Wang Z. L., Wang J., "Improved output performance of direct-current triboelectric nanogenerator through field enhancing breakdown effect", Adv. Mater. Technol. 6, 2100195, (2021).
33. Zhao Z., Liu D., Li Y., Wang Z. L., Wang J., "Direct-current triboelectric nanogenerator based on electrostatic breakdown effect", Nano Energy 102, 107745, (2022).
34. Ma S., Ribeiro F., Powell K., Lutian J., Møller C., Large T., Holbery J., "Fabrication of novel transparent touch sensing device via drop-on-demand inkjet printing technique", ACS Appl. Mater. Interfaces 7, pp. 21628 - 21633, (2015).
35. Yang W., Li N.-W., Zhao S., Yuan Z., Wang J., Du X., Wang B., Cao R., Li X., Xu W., Wang Z. L., Li C., "A breathable and screen-printed pressure sensor based on nanofiber membranes for electronic skins", Adv. Mater. Technol. 3 1700241, (2018).
36. Wang Q., Jian M., Wang C., Zhang Y., "Carbonized silk nanofiber membrane for transparent and sensitive electronic skin", Adv. Funct. Mater. 27, 1605657, (2017).
37. Wang Z.L., Jiang T., Xu L., "Toward the blue energy dream by triboelectric nanogenerator network", Nano Energy 39, pp. 9 - 23, (2017).
38. Fan F. R., Tang W., Wang Z. L., "Flexible nanogenerators for energy harvesting and self-powered electronics", Adv. Mater. 28, pp. 4283 - 4305, (2016).
39. Wu H., Huang Y., Xu F., Duan Y., Yin Z., "Energy harvesters for wearable and stretchable electronics: from flexibility to stretchability", Adv. Mater. 28, pp. 9881 - 9919, (2016).
40. Wang J., Wu C., Dai Y., Zhao Z., Wang A., Zhang T., Wang Z. L., "Achieving ultrahigh triboelectric charge density for efficient energy harvesting, Nat. Commun. 8, p. 88, (2017).